Photodecomposition of natural organic metal-binding ligands from deep seawater

Mitsuhide Sato[a*], Natsuki Ogata[b], Kuo Hong Wong[c], Hajime Obata[c] and Shigenobu Takeda[a]

[a] Graduate School of Fisheries and Environmental Sciences, Nagasaki University, 1-14, Bunkyo-machi, Nagasaki-shi, Nagasaki, 852-8521 Japan

[b] Faculty of Fisheries, Nagasaki University, 1-14, Bunkyo-machi, Nagasaki-shi, Nagasaki, 852-8521 Japan

[c] Atmospheric and Ocean Research Institute, The University of Tokyo, 5-1-5, Kashiwanoha, Kashiwa-shi, Chiba, 277-8564 Japan

[*] Corresponding author: 310mitsuhide@gmail.com

16   Abstract

17   To reveal the effect of solar irradiation on the biogeochemical cycling of trace metals in

18   the open ocean, the photodecomposition of organic iron- and copper-binding ligands

19   was examined in an experiment using filtered seawater collected from a deep layer of

20   the East China Sea. Six days of natural solar irradiation caused a significant decrease in

21   the concentrations of both ligands, along with the loss of fluorescent dissolved organic

22   matters. The relative decrease of iron-binding ligands, which are considered to be

23   mainly composed of humic substances, was larger than that of copper-binding ligands or

24   humic-like fluorescence. This may be attributable to relatively high photoreactivity of

25   hydrophilic fluvic acids, which have higher affinity to ferric ions. Surprisingly, an

26   accumulation of both iron- and copper-binding ligands was observed in the dark control

27   bottles, but without a significant change in the fluorescence of humic-like substances. In

28   conclusion, the upwelling of deep seawater into the sunlit surface layer can result in the

29   rapid loss of the complexation capacity for both iron and copper ions. The stronger

30   ligands for both metals, which were readily decomposed by sunlight irradiation, appears

31   to have a similar composition, suggesting that competition could be important to

32   determine the solubility and bioavailability of iron and copper.

33   Keywords: Iron; copper; ligands; humic substances

34

35 Introduction

36   The biogeochemical cycling of trace metals, including iron (Fe), copper (Cu), zinc

37 (Zn), and cobalt (Co) in the ocean is tightly coupled with that of dissolved organic

38 matter. This is because most trace metal ions in seawater exist as complexes with

39 organic ligands (Fe: Gledhill and Buck, 2012; Cu: Moffett and Dupont, 2007; Whitby et

40 al., 2018; Zn: Ellwood and van den Berg, 2000; Kim et al., 2015b; Co: Ellwood et al.,

41 2005; Noble et al., 2017). Organic complexation plays a pivotal role in stabilizing trace

42 metal ions in the dissolved phase. For example, Fe, which is an essential element for

43 most organisms, is virtually insoluble as an inorganic ion in oxygenated seawater and

44 can be present at a concentration as low as 0.1 nM (Liu and Millero, 2002). In

45 oversaturated conditions, Fe can be readily removed from seawater via the formation of

46 colloids and particles. Organic ligands, on the other hand, help ferric ions (Fe^{3+}) to

47 remain in solution in the water column (Kuma et al., 1998), thus making them available

48 for subsequent biological uptake.

49   Among all of the trace metals, Fe and Cu are of notable importance for biological

50 production and the recycling of carbon in seawater. Both metals are essential elements

51 for every organism, and are particularly required by photosynthetic organisms.

52 Dissolved Fe can be depleted in the surface water of the open ocean to a level that can

53 limit primary production (Martin et al., 1994; Boyd et al., 2000; Tsuda et al., 2003).

54 Some reports have suggested that the primary production of some phytoplankton may

55 also be limited by Cu deficiency (Maldonado et al., 2006).

56   Organic complexation has a profound influence on the biological uptake of trace

57 metal ions in seawater as well as their stability in the water column. Although a detailed

58 chemical inventory of organic Fe-binding ligands in seawater has yet to be reported,

59   siderophores, humic substances, and microbial exopolymeric substances (porphyrins,

60   saccharides, and humic-like substances) have been proposed as possible ligands

61   (Hassler et al., 2017). Different ligands exhibit different complexation, dissociation, and

62   biological uptake mechanisms; hence, they have varying affinities for Fe^{3+}. This means

63   that the bioavailability of Fe complexed with different ligands varies, which can also

64   further depend on the target organism. For example, Fe complexed with siderophores, a

65   compound released by bacteria to specifically incorporate low concentrations of Fe^{3+}, is

66   less available to eukaryotic phytoplankton than to prokaryotic cyanobacteria (Hutchins

67   et al., 1999). This means that understanding the composition of organic ligands as well

68   as their concentration is essential to elucidate the biogeochemical cycling of trace

69   metals.

70   The organic complexation of Cu ions also controls the bioavailability of Cu to

71   microbes. It is known that organic Cu-binding ligands are mainly composed of protein-

72   based phytoplankton exudates, thiols, and humic substances (Dupont et al., 2006;

73   Laglera and van den Berg, 2009; Leal and van den Berg, 1998; Whitby and van den

74   Berg, 2015). These are particularly rich in estuarine and coastal waters, which can

75   maintain the stability of Cu ions in the water column. Although Cu is an essential

76   element for every organism, a surplus of free cupric ions (Cu^{2+}) is toxic to microbes

77   (Coale, 1991). A high input of Cu into the ocean may control the composition and

78   growth of the natural phytoplankton community in some areas (Paytan et al., 2009).

79   Organic Cu-binding ligands buffer the toxicity of free Cu^{2+} through complexation.

80   Understanding the sources and sinks of organic trace-metal binding ligands and trace

81   metals is key for revealing the biogeochemical cycling of trace metals. Organic metal-

82   binding ligands are mainly supplied to the ocean through riverine discharge,

83   atmospheric deposition, hydrothermal vents, biological production/excretion, and the

84   microbial decomposition of organic materials (Gledhill and Buck, 2012; Hassler et al.,

85   2017). On the other hand, metal-binding ligands can be decomposed via biological

86   processes operating throughout the water column as well as by photodegradation in the

87   sunlit surface water. In the surface mixed-layer, where biological production occurs,

88   photodecomposition by solar irradiation is considered to be a main sink of organic trace

89   metal-binding ligands (Hassler et al., 2017).

90   The photodecomposition of organic Cu-binding ligands has been investigated in

91   estuarine waters (Laglera and van den Berg, 2006; Shank et al., 2006). As a significant

92   fraction of the organic Cu-binding ligands in the ocean is composed of humic

93   substances, their photochemistry has been studied in relation to humic substances

94   (Vidali et al., 2010; Tonietto et al., 2011), which have a high photoreactivity (Kulovaara

95   et al., 1996). These previous studies demonstrated that solar radiation can result in the

96   rapid decomposition of humic substances. However, there are still few studies regarding

97   the photoreactivity of Cu-binding ligands in the marine environment, especially in the

98   open ocean (Moffett et al., 1990).

99   The photochemistry of purified siderophores has been relatively well studied

100   (Barbeau, 2006), whereby their photoreactivity is understood to depend on their

101   chemical form and binding state. However, Fe-binding ligands in natural seawater are a

102   mixture of various chemical forms, and siderophores occupy only a small fraction of

103   Fe-binding ligands in natural seawater (Hassler et al., 2017). Further, some field

104   experiments have yielded inconsistent outcomes, for example, rapid

105   photodecomposition was observed in the Gulf of Mexico (Powell and Wilson-Finelli,

106   2003), whereas no discernible change was found in Dutch estuaries (Rijkenberg et al.,

107 2006). This is probably partly due to the different compositions of Fe-binding ligands in

108 different areas. As organic ligands may have unique geographical features, there is a

109 need to reveal the photoreactivity of organic ligands in various marine environments.

110   In the present study, we focus on the photoreactivity of organic Fe- and Cu-binding

111 ligands within water samples collected from depth in the East China Sea. Deep seawater

112 was selected as the research object for the following two reasons. First, deep seawater

113 contains a different composition of organic metal-binding ligands than that in ocean

114 surface waters or estuarine seawater. Recent studies suggested that the contribution of

115 humic substances to Fe complexation may increase in the deep water of the open ocean

116 (Kitayama et al., 2009; Hassler et al., 2017). As mentioned previously, the high

117 photoreactivity of humic substances can affect the complexing capacities of trace metals

118 in seawater. Second, deep water upwelling is one of the principal supply pathways of

119 trace metals to the surface mixed layer (e.g. Nishioka et al., 2020), whereby trace metals

120 are supplied with organic ligands that occur in deep water. Therefore, revealing the

121 photochemical reaction of organic ligands to sunlight is essential to determine the fate

122 of trace metals supplied to the surface layer. However, because the photoreactivity of

123 organic trace metal ligands from deep water is currently unknown, we conducted a

124 sunlight irradiation experiment using deep seawater collected from the East China Sea

125 to investigate this aspect.

126

127 Materials and Methods

128 <u>Sampling</u>

129   The seawater for the irradiation experiment was collected at Station G1 (32°09′N,

130 129°11′E, bottom depth: 563 m) aboard T/S Kakuyo-maru in on 21 August 2019.

131 Vertical profiles of temperature, salinity, and chlorophyll *a* fluorescence were obtained

132 from a CTD instrument (SBE-911plus, Sea-Bird Scientific) and Seapoint Chlorophyll

133 Fluorometer (Seapoint Sensors, Inc.) installed on a rosette sampler with X-type Niskin

134 samplers acid-cleaned according to Kim et al. (2015b), which were suspended by a

135 stainless steel-armored cable. The CTD sensor have been annually calibrated by the

136 manufacturer. Samples for the analysis of fluorescent dissolved organic matter (FDOM)

137 were collected from different depths using the Niskin samplers. Seawater for the

138 photodecomposition experiment was collected from a depth of 554 m., about 9 m above

139 the bottom of the sea.

140 FDOM

141 The samples for the analysis of FDOM were collected using polypropylene syringes,

142 which had been rinsed with Milli-Q water (> 18.2 MΩ cm) after soaked in 1.2 N HCl

143 overnight. The samples were filtered directly through pre-combusted GF/F Whatman

144 filters that were set on a filter holder connected to the syringe. Then, approximately 20

145 mL of each aliquot was dispensed into a pre-combusted (450 °C for 3 h) 30-mL amber

146 glass vial. The filtrates were stored frozen (−20 °C) awaiting analysis on-land.

147 In the laboratory on land, these samples were first thawed in the dark at room

148 temperature before analysis using a spectrofluorometer. The 3-D excitation emission

149 spectrum matrix was obtained for each sample for excitation and emission ranges from

150 225 nm to 400 nm (5 nm intervals) and 225 nm to 507 nm (1 nm interval), respectively,

151 using a spectrofluorometer (HITACHI F-2700) (Yamashita and Tanoue, 2003). The

152 response time was set to 0.08 s when the scan speed was 1500 nm min^{-1}. The

153 fluorescence intensity was normalized to the integral intensity of Raman scattering for

154 Milli-Q water at an emission range of between 365 nm to 450 nm (1 nm interval) with a

155 350 nm excitation wavelength expressed in Raman units (RU). A PARAFAC analysis

156 for peak identification was run on MATLAB R2014a (MathWorks) and

157 DOMFluortoolbox (Stedmon and Bro, 2008). The vertical profile samples and samples

158 from the photodecomposition experiment were analyzed together, which included the

159 samples collected from the other stations during the cruise, and the total number of

160 sample was 133. Four peaks were identified, which were attributed to humic substances

161 of terrestrial and marine origins, and tryptophan-like and tyrosine-like proteins,

162 respectively, according to Yamashita and Tanoue (2003).

163 <u>Photodecomposition experiment</u>

164   The response of FDOM and metal-binding ligands to natural sunlight was examined

165 by the natural sunlight irradiation experiment as shown in Fig. 1. The deep seawater

166 collected for the photodecomposition experiment was dispensed into 24 500-mL Teflon

167 FEP bottles (Nalgene), which had been washed by heating in a mixture of concentrated

168 nitric, sulfuric and perchloric acid, 6 M hydrochloric acid, and Milli-Q water as

169 previously described (Obata et al., 1993). The samples were filtered through an AcroPak

170 capsule filter with a nominal pore size of 0.2 μm that was directly connected to a Teflon

171 spigot of the Niskin sampler. Before use, the capsule filter was filled by 0.05 N HCl

172 (metal analysis grade) overnight at 60°C, thoroughly rinsed with Milli-Q water and then

173 filled by Milli-Q water overnight at 60°C, followed by thorough rinsing with Milli-Q

174 water to minimize the possible contamination of metals and organic materials (Yoro et

175 al., 1999). All filtrates were stored in the dark with ice packs to minimize the effects of

176 light and temperature. Two days after collection, all of the bottles were transferred to the

177 rooftop of a building in Nagasaki University for the experiment. Six bottles were

178 wrapped with aluminum foil for the dark control. The bottles were placed in a

179   temperature-controlled (25 °C) water tank under non-attenuated sunlight. While the air

180   temperature fluctuated between 20 and 30 °C during the experiment, the water

181   temperature was maintained between 25 and 26 °C. The experiment continued for 6

182   days, and six bottles were recovered on days 0, 1, and 6. The dark control bottles were

183   recovered after 6 days. Solar irradiation was monitored by measuring the downward

184   flux of 400–700 nm irradiation with a cosine-type quantum sensor (DEFI-L, JFE

185   Advantec). With the exception of the final day of the experiment, it was overcast during

186   the experiment, and the maximum daytime PAR flux was approximately 500 μmol m^{-2}

187   s^{-1}.

188   For the analysis of FDOM, 30 mL aliquots were dispensed into pre-combusted 30-

189   mL amber glass bottles from each of the six bottles. All of the remaining seawater

190   samples were stored at −20 °C awaiting trace metal and ligand analysis. Three of the

191   bottles were used for dissolved Fe and organic Fe-binding ligand analyses, while the

192   other three were used for Cu and organic Cu-binding ligand analyses.

193   <u>Dissolved Cu and Fe concentrations</u>

194   The total dissolved Cu and Fe concentrations were determined using cathodic

195   stripping voltammetry (CSV) following the protocol described (Campos and van den

196   Berg, 1994 and Abualhaija and van den Berg, 2014, respectively), after the seawater

197   samples were exposed to UV-irradiation. For Cu measurement, acidified seawater

198   samples were first UV-irradiated for 60 min in Teflon beakers covered by quartz caps

199   (Kim et al., 2015a). After neutralization with 25 μL of 20% ammonia solution

200   (Tamapure AA-100, Tama Chemicals), 10 mL of each UV-irradiated sample was

201   pipetted into the voltammetric cell and spiked with 25 μL of 10 mM salicylaldoxime

202   (SA, Aldrich, >98.0%) and 100 μL of 1 M borate buffer. For Fe samples, the seawater

203   was UV-irradiated by a flow-through irradiation system with twin 15-V UV lamps (VL-

204   215, Vilber Lourmat) followed by overnight cooling. After that, 10 mL of the aliquot

205   was spiked with 100 µL of 1 M borate buffer and 50 µL of 1 mM SA solution.

206   For Cu measurement, a 797 VA Computrace (Metrohm) voltammetric system was

207   used. A glassy carbon rod and Ag/AgCl with a 3 M NaCl salt bridge were used for the

208   auxiliary and reference electrodes, respectively. Each aliquot was transferred to a Teflon

209   sample cell and purged with N_2 gas (99.9995%) for 180 s before analysis. During

210   deposition, the sample was stirred using a magnetic stirrer at 2000 rpm. The mercury

211   size was set to 8.

212   The reduction current of Fe-SA complexes was measured by a controlled growth

213   mercury electrode cell stand (BASi) connected to a laptop PC. For the auxiliary and

214   reference electrodes, platinum wire (0.5 mm diameter) and Ag/AgCl with a 3M NaCl

215   salt bridge were adopted, respectively. Each aliquot was transferred to a Teflon sample

216   cell and saturated with filtered clean air (Air Liquide Japan) for 120 s before analysis.

217   Fe-SA complexes were deposited on a mercury drop (drop size = 16) while stirred using

218   a magnetic stirrer at 600 rpm.

219   The voltammetric parameters were listed in Table 1. The analyses were repeated

220   three times for each sample. The total Cu and Fe concentrations were calibrated by the

221   addition of standard solution prepared by diluting atomic absorption spectrometry

222   standard $Cu(NO_3)_2$ and $Fe(NO_3)_3$ solutions, respectively.

223   <u>Titration of Cu- and Fe-binding ligands</u>

224   The concentrations and conditional stability constants of Cu- and Fe-binding organic

225   ligands were determined using competitive ligand-exchange adsorptive CSV (CLE-

226   AdCSV). Detailed descriptions of this method can be found elsewhere (Campos and van

227   den Berg, 1994; Abualhaija and van den Berg, 2014). Briefly, a ligand titration consisted

228   of 15 and 12 Teflon vials for Cu and Fe ligands, respectively. In each vial, 10 mL of

229   seawater sample, 100 μL of 1 M borate buffer (pH 8.2), and Cu (0 -30 nM) or Fe (0 -7

230   nM) were added. After equilibration (1 h for Cu, 2 h for Fe), 5 μM of SA was added to

231   each vial as the competing ligand, and the vials were then left to equilibrate. The

232   equilibration time was overnight and > 3 h for Cu- and Fe-binding ligands, respectively.

233   For Cu-binding ligands, the first preparation of the titration was carried out to

234   'condition' the vials and was subsequently discarded. For Fe-binding ligands, Teflon

235   jars were preconditioned by repeating these procedures three times using UV-irradiated

236   surface seawater sampled from the Pacific Ocean. The titration procedure was repeated

237   using the same vials, and the concentration of metal-SA complexes in each vial was

238   measured using CSV. The voltammetric parameters were the same as those used to

239   determine the total dissolved Cu or Fe concentration (Table 1). Deposition and scanning

240   were repeated twice for each aliquot. All the procedures were made in a class-1000

241   clean room pressurized with air processed through a HEPA filter.

242   Peak reduction current values were plotted against the total dissolved metal

243   concentration (i.e., the sum of the dissolved Cu or Fe concentration in the unamended

244   seawater plus the added metal concentration). The titration data were then analyzed

245   using the metal complexation calculation software ProMCC (Omanović et al., 1995).

246   For Cu, two types of ligands, the strong and weak Cu-binding ligands (CuL_1 and CuL_2,

247   respectively), were assumed. For Fe, as there was no apparent kink or curvature point

248   on the plot, we fitted the titration data using non-linear fitting models on the assumption

249   that all of the samples contained only one type of FeL within the detection window.

250   The concentration of metal-binding ligands is expressed as a molar equivalent

251   concentration of binding metal ions (nmol L^{-1}). Statistical tests were performed using

252   OriginPro (OriginLab). Differences between days or treatments were tested using the

253   Tukey–Kramer method.

254

255   Results and Discussion

256   <u>Hydrography and field data</u>

257   Hydrography data revealed that the sampling station G1 was affected by riverine

258   input down to a depth of 25 m, as evidenced by the layer with a high temperature and

259   reduced salinity (Fig. 2A). The temperature decreased towards the bottom, while

260   salinity peaked at a depth of ~80 m. Chlorophyll-*a* fluorescence showed a subsurface

261   maximum at a depth of ~60 m. The entire water column was highly stabile, which is

262   typical for the East China Sea during the summer.

263   Of the four identified types of FDOM, tryptophan-like proteins were relatively

264   scarce and their fluorescence intensity was highly variable; thus, we only present the

265   data for the other three types of FDOM in this report: terrestrial humic-like substances

266   (THS), marine humic-like substances (MHS), and tyrosine-type protein-like substances

267   (TYR) (Fig. 1B). Of these, THS and MHS exhibited similar vertical distributions, with

268   relatively low fluorescence intensities in the low-salinity surface layer down to 25 m.

269   Below 25 m, the fluorescence intensity of THS slightly increased towards the sea

270   bottom, especially below 300 m, whereas the MHS fluorescence intensity was relatively

271   constant. In contrast, the fluorescence intensity of TYR was high in the low-salinity

272   surface water and low in the deep water (Fig. 2B).

273   These contrasting distribution patterns of humic-like and protein-like substances

274   have implications for their origin and decomposition processes. The nutrient-like pattern

275   of humic-like substances suggests that they were produced in deep water, probably

276   through microbial processes. The net production of humic substances by natural

277   assemblages (Kramer and Herndl, 2004) or isolated cultures (Shimotori et al., 2012) of

278   marine heterotrophic bacteria has been shown previously. In addition to autochthonous

279   production, THS is likely transferred from a terrestrial origin to deep water via the

280   thermohaline circulation. We note that we use the terms 'terrestrial' and 'marine' as

281   nominal categories based on the fluorescence properties, which are not necessarily

282   consistent with the actual origins. The low fluorescence of humic-like substances in the

283   surface layer could be attributed to their low supply from riverine sources and/or

284   photodecomposition. In the present study, the latter should be more significant because

285   during the same cruise, humic-like substances were found to be more abundant at the

286   coastal sampling stations, which were more affected by riverine water inputs. Thus, at

287   the sampling station in the present study, the surface water is considered to have

288   experienced irradiation sufficient to decompose photoreactive DOM. On the contrary, a

289   high abundance of protein-like substances in the low-salinity surface water suggests that

290   these substances were transferred from riverine water and/or produced through

291   photosynthesis by phytoplankton. Therefore, DOM and organic metal-binding ligands in

292   the surface water were likely dominated by biologically "labile" components, as

293   proposed by Hassler et al. (2020).

294   Changes in FDOM and metal-binding ligands during the photodecomposition

295   experiment

296   During the 6-day experiment with natural sunlight irradiation, the fluorescence of all

297   three types of FDOM exhibited a constant reduction (Fig. 3A). In the dark control

298   bottles, there was no significant change in the FDOM fluorescence after 6 days of

299 incubation, thus indicating that thermodynamic decomposition or aggregation was

300 negligible. Out of the three types of FDOM, THS showed the fastest

301 photodecomposition, with the fluorescence decreasing by 20% on day 1 of the

302 incubation, although it was overcast and the sunlight was relatively weak during the

303 first five days of the experiment. In contrast, the decrease in the fluorescence on day 1

304 was not significant for MHS and TYR ($p < 0.05$). After 6 days of incubation, the

305 relative decrease to the initial fluorescence was 42%, 23%, and 19% for THS, MHS,

306 and TYR, respectively.

307 The seawater used for the irradiation experiment contained 2.08±0.13 and 0.25±0.03

308 nM of dissolved Cu and Fe, respectively, both of which were within the range of the

309 values observed in the deep layers of the East China Sea (Sasayama et al., 2018; Wong

310 et al., 2019). Using these figures and the titration data, the initial concentrations of

311 CuL_1, CuL_2, and FeL were calculated to be 1.85±0.05, 4.93±1.83, and 1.17±0.09 nM,

312 respectively. The changes in the concentrations of CuL_1, CuL_2, and FeL during the 6-

313 day experiment were completely different from those of FDOM (Fig. 3B). On day 1, the

314 concentrations of all three ligands showed subtle increases that were not statistically

315 significant. After 6 days of solar irradiation, CuL_1 and FeL decreased by 26% and 53%,

316 respectively, as compared to those before the incubation. In contrast, CuL_2 increased by

317 three times that of the initial sample, although the variance among replicates was large

318 (~127% of the mean initial value) and the increase was not statistically significant ($p >$

319 0.05). It is notable that there was a marked increase in the concentration of all three

320 ligands in the dark control bottles after 6 days of incubation; however, this was only

321 statistically significant for FeL ($p < 0.05$). As CuL_1 was not detected in one of the

322 triplicates of the dark control, a statistical test was not applied for CuL_1.

323   The conditional stability constants of organic metal-binding ligands are indices of

324   their affinity to metal ions. These changed less dramatically during the

325   photodecomposition experiment in comparison to the changed observed in the

326   concentrations of CuL_1, CuL_2, and FeL (Table 1). The affinity of CuL_1 to Cu^{2+} was two

327   orders of magnitude higher than that of CuL_2. The stability constant of CuL_1

328   significantly decreased after 6 days of solar irradiation ($p < 0.05$), as compared with day

329   0 and dark control. For CuL_2, the deviation among replicates was large and no

330   discernible trend was observed. The conditional stability constant of FeL was

331   approximately 10^{11} M^{-1}, thus corresponding to 'weak' Fe-binding ligands, which have

332   been reported to occur in the deep water of the Pacific Ocean (Rue and Bruland, 1995;

333   Kondo et al., 2012; Buck et al., 2018).The conditional stability constant of FeL was

334   significantly higher on day 6 than on day 0 and in the dark control ($p < 0.05$). The

335   changes in the conditional stability constants (Table 1) demonstrate that FeL with

336   relatively low affinity to Fe^{3+} were decomposed by sunlight, whereas a strongly bound

337   fraction of CuL_1 was decomposed.

338   Taking the relatively weak irradiation during the experiment and light attenuation by

339   Teflon bottles into account, the present results demonstrate that FeL from deep seawater

340   are decomposed by natural sunlight on a daily scale. This is consistent with a recent

341   report that the organic materials extracted from deep seawater lost their Fe complexing

342   capacity after exposure to simulated sunlight (Hassler et al., 2020). This is in contrast to

343   the results for FeL in the surface water, where no discernible change was observed after

344   UV irradiation (Rijkenberg et al., 2006). This is probably because the surface water

345   contains a small amount of photoreactive FeL, due to rapid photodecomposition of

346   photoreactive FeL as observed in our present study.

347   The relative changes in the fluorescence intensities of the three types of FDOM and

348   the ligand concentrations during the photodecomposition experiment were compared

349   (Fig. 4). As mentioned, THS, MHS, TYR, CuL_1, and FeL all decreased during 6 days of

350   solar irradiation in comparison to their initial values and the dark control; however, the

351   individual patterns clearly differed. The most important points are that (1) THS and FeL

352   decreased most rapidly of all the five components, and (2) the two metal-binding

353   ligands were decomposed by solar irradiation, although the net increase in the dark

354   control suggests that they were probably also simultaneously produced.

355   The rapid photodecomposition of FDOM, especially humic-like substances, from

356   deep seawater has been previously reported (Timko et al., 2015; Cao et al., 2020; Yang

357   et al., 2020). Further, a higher photoreactivity of terrestrial humic substances in

358   comparison to marine humic substances was reported for the northern Sargasso Sea

359   (Timko et al., 2015), which could have resulted from differences in chemical forms. The

360   vertical profiles of humic-like substances (Fig. 2B) suggest that it is unlikely that

361   humic-like substances occurring in the experimental seawater originated directly from a

362   riverine source. It is more likely that they were produced through heterotrophic

363   processes by autochthonous microbes (Kramer and Herndl, 2004; Nieto-Cid et al.,

364   2006; Shimotori et al., 2009) or transported via thermohaline cycling. The production of

365   humic-like substances by microbes is also suggested by its good correlation with AOU

366   in the western North Pacific (Kitayama et al., 2009). On the other hand, in the

367   Mediterranean Sea, electrochemically determined concentration of humic-like

368   substances was negatively correlated with AOU, suggesting that degradation by

369   heterotrophic bacteria seemed to be a main sink of humic ligands in the deep sea

370   (Dulaquais et al., 2018). This discrepancy may be attributable to differences in the study

371 region (Pacific vs. Mediterranean) or methodology (fluorometry vs. voltammetry), and

372 the present results are considered to be comparable with the case in the North Pacific.

373   A lower photoreactivity of protein-like FDOM in comparison to humic-like

374 substances (Figs. 3A and 4) has been reported in previous studies (Timko et al., 2015;

375 Yang et al., 2020). This difference in photoreactivity could explain their differential

376 vertical distributions, in which humic-like substances are enriched in deep water,

377 whereas protein-like substances are abundant in surface sunlit water (Cao et al., 2020).

378 <u>Sunlight-induced changes in metal-binding ligands from deep water</u>

379   One of the most important findings in the present experiment is that FeL and CuL_1

380 reacted similarly to natural solar irradiation (Fig. 3B); the concentrations of both ligands

381 substantially decreased during the 6 days of irradiation, whereas they accumulated in

382 the dark control bottles. It is unlikely that this was due to any experimental artifact

383 because the samples for FeL and CuL were derived from separate triplicate bottles (see

384 Materials and Methods) and were analyzed by different researchers using different

385 instruments. Therefore, the present results strongly suggest that both ligands possessed a

386 similar photoreactivity. It is also possible that some portion of the Fe^{3+} and Cu^{2+} in the

387 deep seawater may have been complexed with common organic ligands.

388   Organic Cu-binding ligands in seawater are mainly composed of humic substances

389 and thiols (Le Gall and van den Berg 1988; Kogut and Voelkler, 2001; Whitby and van

390 den Berg, 2015). In relation to this, the photoreactivity of strong organic Cu-binding

391 ligands has been studied in various situations (Laglera and van den Berg, 2006; Shank

392 et al., 2006), whereby their concentrations were found to decrease after irradiation,

393 which is consistent with the results of the present study.

394   It has been proposed that organic Fe-binding ligands in seawater are a complex

395   mixture of various types of organic matter, including siderophores, humic substances,

396   and biological excretion products (e.g., exopolymer substances and polysaccharides)

397   (Hassler et al., 2017). In the present study, the contribution of siderophores to FeL is

398   considered to be minor because the experimental seawater was collected from a

399   relatively Fe-rich (> 0.2 nM) deep layer. The relatively low conditional stability

400   constant ($\sim 10^{11}\,M^{-1}$, Table 1) also supports a minor contribution of siderophores to Fe

401   complexation. It is known that humic substances play an important role in Fe

402   complexation in estuary systems, where the riverine load of both Fe and humic

403   substances is substantial (Krachler et al., 2015). However, the findings of recent field

404   surveys suggested that humic substances in deep water could control Fe complexation

405   even in the open ocean (Laglera and van den Berg, 2009; Heller et al., 2013; Whitby et

406   al., 2020). It has been estimated that humic substances account for between $\sim$20% to

407   60% of the electrochemically measured Fe-binding capacity (Dulaquais et al., 2018;

408   Whitby et al., 2020). The present finding that some fraction of the FeL from the deep

409   seawater was decomposed by natural solar irradiation (in proportion to CuL$_1$) agrees

410   with the significant contribution of humic substances to Fe complexation. Moreover, the

411   range of the conditional stability constant ($K_{Fe'L}$) ($10^{10.8}$ to $10^{11.6}\,M^{-1}$; Table 1) in this

412   study was of a similar range to that previously reported for humic substances in

413   seawater ($10^{10.6}$ to $10^{11.1}\,M^{-1}$; Laglera and van den Berg, 2009). The relatively high

414   conditional stability constant of CuL$_1$ is consistent with reported $K_{Cu'L}$ values of humic-

415   like substances (Whitby and van den Berg 2015).

416   However, some caution is required when relating the fluorometrically measured

417   humic-like substances with electrochemically measured metal-binding ligands. The

418   decrease in fluorometrically determined FDOM is due to the photodegradation of the

419   fluorophores, which is not accompanied by decrease in total amount of DOC (Omori et

420   al., 2015). Similarly, the decrease of electrochemically determined metal-binding

421   ligands means the loss of binding capacities of ligand molecules, not remineralization of

422   the molecules. Considering that aromatic rings, which are preferentially decomposed by

423   photoreaction (Medeiros et al., 2015), play a pivotal role both in fluorescence and ion

424   chelating, these two processes are likely related with each other to some degree.

425   However, we should strictly distinguish these two processes.

426   The net accumulation of FeL and CuL_1 in the dark control, which was not observed

427   for fluorescence of humic-like substances, was noteworthy. By taking the prefiltration

428   through a 0.2-μm filter into consideration, we consider that it was unlikely that there

429   was new microbial production of metal-binding ligands, although concomitant bacterial

430   growth during the 6-day incubation cannot be entirely excluded. On the other hand, it is

431   probable that the temperature increase from 7 °C to 25 °C promoted the production of

432   metal-binding ligands by some thermodynamic processes. However, it is unknown

433   whether this involved decomposition or an aggregation process because we are unaware

434   of any similar reports of such a dark accumulation of organic metal-binding ligands.

435   The increase of CuL_2 in the light and dark bottles (Fig. 3B) may be similarly explained

436   by thermal reactions, although there was a large variance in the CuL_2 concentration

437   among the triplicate samples.

438   Assuming that the accumulation of metal-binding ligands occurred irrespective of

439   light intensity, the gross photodecomposition of organic metal-binding ligands should

440   have been larger than the net decomposition in Fig. 4. However, a precise estimation of

441   the gross photodecomposition is difficult in the present experiment because it is

442   unknown whether the accumulation was promoted or suppressed under solar irradiation.

443   In any case, short-duration solar radiation experiments using a solar simulator or UV

444   lamp may overestimate the daily net decomposition of organic ligands. The rapid

445   photodecomposition of organic Fe-binding ligands in surface seawater during the

446   daytime (Powell and Wilson-Finelli, 2003) may be partly compensated for by a similar

447   process.

448   The absence of a net accumulation of FDOM in the dark control bottles suggests that

449   the metal-binding ligands produced in the dark were non-fluorescent compounds that

450   probably differed to those that originally occurred in the deep seawater, and were

451   decomposed by solar irradiation. This suggests that the solar irradiation of the deep

452   seawater changed the chemical compositions of the organic metal-binding ligands more

453   than their concentrations. Although the photoreactivity of the ligands produced in the

454   dark was not examined in the present study, it is possible that some of them were

455   tolerant to solar irradiation and remained as recalcitrant organic matter. It will be an

456   important step to reveal the fate of dissolved Fe in seawater that has upwelled from the

457   deep ocean to the surface waters.

458   When taken together, the parallel changes in the concentrations of FeL and CuL_1

459   (Fig. 3B) in response to solar irradiation strongly support high photoreactivity of

460   organic metal-binding ligands collected from the deep water. The photoreactive ligands

461   likely include fluorescent humic-like substances, some fraction of which may be bound

462   to both Cu^{2+} and Fe^{3+} (Abualhaija et al., 2015; Whitby and van den Berg, 2015; Whitby

463   et al., 2018; 2020), and the loss of their complexing capacity may be related with the

464   loss of fluorescence of the humic-like substances. The loss of fluorescence and binding

465   capacities were likely invoked by light-induced decomposition of polycyclic aromatics

466   (Medeiros et al., 2015). However, it is unlikely that Cu^{2+} and Fe^{3+} compete for the

467   totally same coordinate positions of the same molecules of humic-like substances,

468   owing to different affinity of Cu^{2+} and Fe^{3+} to different types of humic-like substances

469   (Yang and van den Berg, 2009; Muller and Cuscov 2017). Fe^{3+} has more affinity to the

470   more acidic hydrophilic fluvic acids (Nuzzo et al., 2013), whereas Cu^{2+} make strong

471   complexes with the less acidic and hydrophobic humic acids (McElmurry et al., 2010).

472   This difference may explain a relatively faster decomposition of FeL compared to CuL_1

473   (Fig. 4), because fluvic acids are more readily degraded by sunlight than humic acids

474   (Kulovaara 1996), which is consistent with stronger photoreactivity of FDOM in the

475   hydrophobic fraction (Omori et al., 2015). In addition to differential photoreactivity of

476   humic-like substances, the fact that CuL_1 include other compounds such as thiols

477   (Laglera and van den Berg 2003) may account for relatively slower decomposition of

478   CuL_1 as compared to FeL.

479   When competition between Fe^{3+} and Cu^{2+} occurs for the same ligands, the

480   equilibrium between free ions and complexation moves toward the free ions, as

481   compared with a single ion model. This may result in more dissociation of Fe^{3+} from the

482   ligands, because the $K_{Fe'L}$ was much lower than the $K_{Cu'L}$ (Table 1), as seen previously

483   (Yang and van den Berg, 2009). Therefore, when competition for ligands occurs,

484   photodecomposition of the ligands can facilitate the formation of Fe colloids more

485   readily than that predicted from a single ion model. To quantify the effect of solar

486   irradiation on the speciation of Fe and Cu in future studies, the concentrations and

487   stability constants of humic substances complexed with Fe^{3+} and Cu^{2+} will be required.

488   Moreover, the photoreactivity of organic Fe-binding ligands is known to change

489   according to their complexation status. For example, catecholate-type siderophores lose

490   their photochemical reactivity when complexed with Fe^{3+}, whereas α-hydroxy

491 carboxylate siderophores are more photoreactive when occurring as a free ligand

492 (Barbeau et al., 2003). Terrestrial humic substances become more refractory to UV

493 irradiation when complexed with excess Cu^{2+} (Liao et al., 2001). Assuming a similar

494 change in photoreactivity, the photodecomposition of metal-binding ligands is likely

495 decelerated, as the decomposition proceeds and the proportion of free ligands decreases.

496

497 Conclusions

498   The findings of the present study clearly demonstrated that, over the 6-day

499 incubation experiment, natural sunlight could decompose the organic Fe-binding ligands

500 and strong Cu-binding ligands within deep seawater. The complexing capacities of the

501 two ligands decreased in parallel with fluorescence of humic-like substances, which are

502 considered to be a main component of metal ligands in the deep seawater. Therefore, it

503 is highly probable that photoreaction of humic-like substances causes the loss of their

504 ability to make complexes with transient metal ions, as well as the loss of their

505 fluorescence. Therefore, photodecomposition of the ligands that can be complexed with

506 both ions can result in a more rapid release of ions than that estimated by a single ion

507 model. This means that Fe^{3+} can readily form colloids and that Cu toxicity can appear

508 more distinctly. To which degree the competition for different metal ions can affect the

509 chemical speciation of metals during the photodecomposition of ligands should be

510 examined using another approach including electrochemical determination of humic

511 substances. Surprisingly, the accumulation of Fe- and Cu-binding ligands was observed

512 in the dark control bottles. The ligands in the dark control bottles had similar affinities

513 to metal ions to those that were decomposed by solar irradiation. However, there was no

514 significant accumulation of FDOM in the dark control bottles, thus indicating that the

515　newly produced ligands were photochemically different to those in the original

516　seawater. These observations demonstrate that the upwelling of deep seawater to the

517　sunlit surface can result in both quantitative and qualitative changes in organic Fe- and

518　Cu-binding ligands, and consequently, chemical speciation changes of both ions.

519

528

529　References

530　Abualhaija, M.M., van den Berg, C.M.G., 2014. Chemical speciation of iron in seawater

531　　using catalytic cathodic stripping voltammetry with ligand competition against

532　　salicylaldoxime. Mar. Chem. 164, 60-74.

533　Abualhaija, M.M., Whitby, H., van den Berg, C.M.G., 2015. Competition between copper

534　　and iron for humic ligands in estuarine waters. Mar. Chem. 172, 46-56.

535　Barbeau, K., Rue, E.L., Trick, C.G., Bruland, K.W., Butler, A., 2003. Photochemical

536　　reactivity of siderophores produced by marine heterotrophic bacteria and

537　　cyanobacteria based on characteristic Fe(III) binding groups. Limnol. Oceanogr. 48,

538　　1069-1078.

539   Barbeau, K., 2006. Photochemistry of organic iron(III) complexing ligands in oceanic

540   systems. Photochem. Photobiol. 82, 1505-1516.

541   Boyd, P. W., Watson, A.J., Law, C.S., Abraham, E.R., Trull, T., Murdoch, R., Bakker,

542   D.C.E., Bowie, A.R., Buesseler, K.O., Chang, H., Charette, M., Croot, P., Downing,

543   K., Frew, R., Gall, M., Hadfield, M., Hall, J., Harvey, M., Jameson, G., LaRoche, J.,

544   Liddicoat, M., Ling, R., Maldonado, M.T., McKay, R.M., Nodder, S., Pickmere, S.,

545   Pridmore, R., Rintoul, S., Safi, K., Sutton, P., Strzepek, R., Tanneberger, K., Turner,

546   S., Waite, A., Zeldis, J., 2000. A mesoscale phytoplankton bloom in the polar

547   Southern Ocean stimulated by iron fertilization. Nature. 407, 695-702.

548   Buck, K.N., Sedwick, P.N., Sohst, B., Carlson, C.A., 2018. Organic complexation of iron

549   in the eastern tropical South Pacific: Results from US GEOTRACES Eastern Pacific

550   Zonal Transect (GEOTRACES cruise GP16). Mar. Chem. 201, 229-241.

551   Campos, M.L.A., van ven Berg, C.M.G., 1994. Determination of copper complexation in

552   sea water by cathodic stripping voltammetry and ligand competition with

553   salicylaldoxime. Anal. Chim. Acta. 284, 481–496. https://doi.org/10.1016/S0003-

554   2670(00)01353-2

555   Cao, F., Zhu, Y., Kieber, D.J., Miller, W.L., 2020. Distribution and photo-reactivity of

556   chromophoric and fluorescent dissolved organic matter in the Northeastern North

557   Pacific Ocean. Deep-Sea Res. I. 155, 103168.

558   Coale, K.H., 1991. Effects of iron, manganese, copper, and zinc enrichments on

559   productivity and biomass in the sub-Arctic Pacific. Limnol. Oceanogr. 36, 1851–

560   1864.

561   Dulaquais, G., Waeles, M., Gerringa, L. J. A., Middag, R., Rijkenberg, M.J.A., Riso, R.,

562   2018. The biogeochemistry of electroactive humic substances and its connection to

563   iron chemistry in the North East Atlantic and the western Mediterranean Sea. J.

564   Geophys. Res., 123, 5481-5499.

565 Dupont, C.L., Moffett, J.W., Bidigare, R.R., Ahner, B.A., 2006. Distributions of

566   dissolved and particulate biogenic thiols in the subartic Pacific Ocean. Deep-Sea Res.

567   I. 53, 1961–1974.

568 Ellwood, M.J., van den Berg, C.M.G., 2000. Zinc speciation in the northeastern Atlantic

569   Ocean. Mar. Chem. 68, 295–306.

570 Ellwood, M.J., van den Berg, C.M.G., Boye, M., Veldhuis, M., de Jong, J.T.M., de Baar,

571   H.J.W., Croot, P.L., Kattner, G., 2005. Organic complexation of cobalt across the

572   Antarctic Polar Front in the Southern Ocean. Mar. Freshw. Res. 56, 1069-1075.

573 Gledhill, M. Buck, K.N., 2012. The organic complexation of iron in the marine

574   environment: a review. Front. Microbiol. 3, 69-69.

575 Harvey, G., Boran, D., Chesal, L., Tokar, J., 1983. The structure of marine fulvic and

576   humic acids. Mar. Chem. 12, 119–132.

577 Hassler, C.S., van den Berg, C.M.G., Boyd, P.W., 2017. Toward a regional classification

578   to provide a more inclusive examination of the ocean biogeochemistry of iron-

579   binding ligands. Front. Mar. Sci. 4. https://doi.org/10.3389/fmars.2017.00019

580 Hassler, C., Cabanes, D., Blanco-Ameijeiras, S., Sander, S.G., Benner, R., 2020.

581   Importance of refractory ligands and their photodegradation for iron oceanic

582   inventories and cycling. Mar. Freshwater Res. 71, 311-320.

583 Heller, M.I., Gaiero, D.M., Croot, P.L., 2013. Basin scale survey of marine humic

584   fluorescence in the Atlantic: Relationship to iron solubility and H_2O_2. Glob.

585   Biogeochem. Cycles. 27, 88-100.

586 Hertkorn, N., Benner, R., Frommberger, M., Schmitt-Kopplin, P., Witt, M., Kaiser, K.,

587   Kettrup, A., Hedges, J.I., 2006. Characterization of a major refractory component of

588   marine dissolved organic matter. Geochim. Cosmochim. Acta. 70, 2990–3010.

589   https://doi.org/10.1016/j.gca.2006.03.021

590 Hutchins, D.A., Witter, A.E., Butler, A., Luther III, G.W., 1999. Competition among

591   marine phytoplankton for different chelated iron species. Nature. 400, 858-861.

592 Kikuchi, T., Fujii, M., Terao, K., Jiwei, R., Lee, Y.P., Yoshimura, C., 2017. Correlations

593   between aromaticity of dissolved organic matter and trace metal concentrations in

594   natural and effluent waters: A case study in the Sagami River Basin, Japan. Sci. Total

595   Environ. 576, 36–45. https://doi.org/10.1016/j.scitotenv.2016.10.068

596 Kim, T., Obata, H., Gamo, T., Nishioka, J., 2015a. Sampling and onboard analytical

597   methods for determining subnanomolar concentrations of zinc in seawater. Limnol.

598   Oceanogr.: Methods. 13, 30–39. https://doi.org/10.1002/lom3.10004

599 Kim, T., Obata, H., Kondo, Y., Ogawa, H., Gamo, T., 2015b. Distribution and speciation

600   of dissolved zinc in the western North Pacific and its adjacent seas. Mar. Chem. 173,

601   330-341.

602 Kitayama, S., Kuma, K., Manabe, E., Sugie, K., Takata, H., Isoda, Y., Toya, K., Saitoh,

603   S.-i., Takagi, S., Kamei Y., Sakaoka, K., 2009. Controls on iron distributions in the

604   deep water column of the North Pacific Ocean: Iron(III) hydroxide solubility and

605   marine humic-type dissolved organic matter. J. Geophys. Res. 114(C8).

606   https://doi.org/10.1029/2008JC004754

607 Kogut, M.B., Voelker, B.M., 2001. Strong copper-binding behavior of terrestrial humic

608   substances in seawater. Environ. Sci. Technol. 35, 1149–1156.

609   https://doi.org/10.1021/es0014584.

610 Kondo, Y., Takeda, S., Furuya, K., 2012. Distinct trends in dissolved Fe speciation

611   between shallow and deep waters in the Pacific Ocean. Mar. Chem. 134-135, 18-28.

612   Krachler, R., Krachler, R.F., Wallner, G., Hann, S., Laux, M., Cervantes Recalde, M.F.,

613   Jirsa, F., Neubauer, E., von der Kammer, F., Hofmann, T., Keppler, B.K., 2015.

614   River-derived humic substances as iron chelators in seawater. Mar. Chem. 174, 85-

615   93.

616   Kramer, G.D., Herndl, G.J., 2004. Photo- and bioreactivity of chromophoric dissolved

617   organic matter produced by marine bacterioplankton. Aquat. Microb. Ecol. 36, 239-

618   246.

619   Kulovaara, M., 1996. Light-induced degradation of aquatic humic substances by

620   simulated sunlight. Intern. J. Environ. Anal. Chem. 62, 85-95.

621   Kulovaara, M., Corin, N., Backlunda, P., Tervo, J., 1996. Impact of UV_{254}-radiation on

622   aquatic humic substances. Chemosphere. 33, 783-790.

623   Kuma, K., Katsumoto, A., Kawakami, H., Takatori, F. and Matsunaga, K., 1998. Spatial

624   variability of Fe(III) hydroxide solubility in the water column of the northern North

625   Pacific Ocean. Deep Sea Research Part I: Oceanographic Research Papers, 45(1): 91-

626   113.

627   Laglera, L.M., van den Berg, C.M.G., 2003. Copper complexation by thiol compounds in

628   estuarine waters. Mar. Chem. 82, 71-89.

629   Laglera, L.M., van den Berg, C.M.G., 2006. Photochemical oxidation of thiols and copper

630   complexing ligands in estuarine waters. Mar. Chem. 101, 130-140.

631   Laglera, L.M., van den Berg, C.M.G., 2009. Evidence for geochemical control of iron by

632   humic substances in seawater. Limnol. Oceanogr. 54, 610–619.

633   Leal, M.F.C., van den Berg, C.M.G., 1998. Evidence for strong copper(I) complexation

634   by organic ligands in seawater. Aquat. Geochem. 4, 49–75.

635   Liao, C.H., Lu, M.C., Su, S.H., 2001. Role of cupric ions in the H_2O_2/UV oxidation of

636   humic acids. Chemosphere. 44, 913-919.

637   Liu, X. Millero, F.J., 2002. The solubility of iron in seawater. Mar. Chem. 77, 43 - 54.

638   Martin, J.H., Coale, K.H., Johnson, K.S., Fitzwater, S.E., Gordon, R.M., Tanner, S.J.,

639   Hunter, C.N., Elrod, V.A., Nowicki, J.L., Coley, T.L., Barber, R.T., Lindley, S.,

640   Watson, A.J., Van Scoy, K., Law, C.S., Liddicoat, M.I., Ling, R., Stanton, T.,

641   Stockel, J., Collins, C., Anderson, A., Bidigare, R., Ondrusek, M., Latasa, M., Millero,

642   F.J., Lee, K., Yao, W., Zhang, J.Z., Friederich, G., Sakamoto, C., Chavez, F., Buck,

643   K., Kolber, Z., Greene, R., Falkowski, P., Chisholm, S.W., Hoge, F., Swift, R.,

644   Yungel, J., Turner, S., Nightingale, P., Hatton, A., Liss, P., Tindale, N.W., 1994.

645   Testing the iron hypothesis in ecosystems of the equatorial Pacific Ocean. Nature.

646   371, 123-129.

647   Maldonado, M.T., Allen, A.E., Chong, J.S., Lin, K., Leus, D., Karpenko,N., Harris, S.L.,

648   2006. Copper-dependent iron transport in coastal and oceanic diatoms. Limnol.

649   Oceanogr. 51,1729–1743.

650   McElmurry, S.P., Long, D.T., Voice, T.C., 2010. Simultaneous quantification of

651   dissolved organic carbon fractions and copper complexation using solid-phase

652   extraction. Appl. Geochem. 25, 650-660.

653   Medeiros, P.M., Seidel, M., Powers, L.C., Dittmar, T., Hansell, D.A., Miller, W.L., 2015.

654   Dissolved organic matter composition and photochemical transformations in the

655   northern North Pacific Ocean. Geophy. Res. Lett. 42, 863-870.

656   Moffett, J.W., Zika, R.G., Brand, L.E., 1990. Distribution and potential source and sinks

657   of copper chelators in the Sargasso Sea. Deep-Sea Res. A. 37, 27-36.

658   Moffett, J.W., Dupont, C., 2007. Cu complexation by organic ligands in the sub-arctic

659   NW Pacific and Bering Sea. Deep-Sea Res. I. 54, 586–595.

660   Muller, F.L.L., Cuscov, M., 2017. Alteration of the copper-binding capacity of iron-rich

661   humic colloids during transport from peatland to marine waters. Environ. Sci.

662   Technol. 51, 3214-3222.

663   Nieto-Cid, M., Álvarez-Salgado, X.A., Pérez, F.F., 2006. Microbial and photochemical

664   reactivity of fluorescent dissolved organic matter in a coastal upwelling system.

665   Limnol. Oceanogr. 51, 1391-1400.

666   Nishioka, J., Obata, H., Ogawa, H., Ono, K., Yamashita, Y., Lee, K., Takeda, S., Yasuda,

667   I. 2020. Subpolar marginal seas fuel the North Pacific through the intermediate water

668   at the termination of the global ocean circulation. Proceedings of the National

669   Academy of Sciences, 117, 12665-12673.

670   Noble, A.E., Ohnemus, D.C., Hawco, N.J., Lam, P.J., Saito, M.A., 2017. Coastal sources,

671   sinks and strong organic complexation of dissolved cobalt within the US North

672   Atlantic GEOTRACES transect GA03. Biogeosciences. 14, 2715-2739.

673   Obata, H., Karatani, H., Nakayama, E., 1993. Automated determination of iron in

674   seawater by chelating resin concentration and chemiluminescence detection. Anal.

675   Chem., 65, 1524-1528.

676   Omanović, D., Garnier, C. Pižeta, I., 2015. ProMCC: An all-in-one tool for trace metal

677   complexation studies. Mar. Chem. 173, 25–39.

678   https://doi.org/10.1016/j.marchem.2014.10.011

679   Omori, Y., Hama, T., Ishii, M., 2015. Photochemical bleaching of fluorescent dissolved

680   organic matter in the subtropical North Pacific Ocean. Geochem. J. 49, 175-184.

681   Paytan, A., Mackey, K.R.M., Chen, Y., Lima, I.D., Doney, S.C., Mahowald, N., Labiosa,

682   R., Postf, A.F., 2009. Toxicity of atmospheric aerosols on marine phytoplankton.

683   Proc. Natl. Acad. Sci. U.S.A. 106, 4601–4605.

684   Powell, R.T., Wilson-Finelli, A., 2003. Photochemical degradation of organic iron

685   complexing ligands in seawater. Aquat. Sci. 65, 367-374.

686   Rijkenberg, M.J.A., Gerringa, L.J.A., Velzeboer, I., Timmermans, K.R., Buma, A.G.J.,

687   de Baar, H.J.W., 2006. Iron-binding ligands in Dutch estuaries are not affected by

688   UV induced photochemical degradation. Mar. Chem. 100, 11-23.

689   Rue, E.L. Bruland, K.W., 1995. Complexation of iron(III) by natural organic-ligands in

690   the central North Pacific as determined by a new competitive ligand equilibration

691   adsorptive cathodic stripping voltammetric method. Mar. Chem. 50, 117-138.

692   Sasayama, R., Hioki, N., Morita, Y., Isoda, Y., Imai, K., Ooki, A., Kuma, K., 2018.

693   Upward transport of iron at the west shelf edge-slope of the Okinawa Trough in the

694   East China Sea. J. Oceanogr. 74, 367-379.

695   Shank, G.C., Whitehead, R.F., Smith, M.L., Skrabal, S.A., Kieber, R.J., 2006.

696   Photodegradation of strong copper-complexing ligands in organic-rich estuarine

697   waters. Limnol. Oceanogr. 51, 884-892.

698   Shimotori, K., Omori, Y., Hama, T., 2009. Bacterial production of marine humic-like

699   fluorescent dissolved organic matter and its biogeochemical importance. Aquat.

700   Microb. Ecol. 58, 55-66.

701   Shimotori, K., Watanabe, K., Hama, T., 2012. Fluorescence characteristics of humic-like

702   fluorescent dissolved organic matter produced by various taxa of marine bacteria.

703   Aquat. Microb. Ecol. 65, 249-260.

704   Stedmon, C.A., Bro, R., 2008. Characterizing dissolved organic matter fluorescence with

705   parallel factor analysis: a tutorial. Limnol. Oceanogr.: Methods. 6, 572–579.

706   Stuermer, D.H., Harvey, G.R., 1977. The isolation of humic substances and alcohol-

707   soluble organic matter from seawater. Deep-Sea Res. 24, 303–309.

708   https://doi.org/10.1016/S0146-6291(77)80010-6

709 Timko, S.A., Maydanov, A., Pittelli, S.L., Conte, M.H., Cooper, W.J., Koch, B.P.,

710   Schmitt-Kopplin, P., Gonsior, M., 2015. Depth-dependent photodegradation of

711   marine dissolved organic matter. Front. Mar. Sci. 2.

712   https://doi.org/10.3389/fmars.2015.00066

713 Tonietto, A.E., Lombardia, A.T., Vieira, A.A.H., 2011. The effects of solar irradiation on

714   copper speciation and organic complexation. J. Braz. Chem. Soc. 22, 1695-1700.

715 Tsuda, A., Takeda, S., Saito, H., Nishioka, J., Nojiri, Y., Kudo, I., Kiyosawa, H.,

716   Shiomoto, A., Imai, K., Ono, T., Shimamoto, A., Tsumune, D., Yoshimura, T., Aono,

717   T., Hinuma, A., Kinugasa, M., Suzuki, K., Sohrin, Y., Noiri, Y., Tani, H., Deguchi,

718   Y., Tsurushima, N., Ogawa, H., Fukami, K. Kuma K., Saino, T., 2003. A mesoscale

719   iron enrichment in the western Subarctic Pacific induces a large centric diatom bloom.

720   Science. 300, 958-961.

721 Vidali, R., Remoundaki, E., Tsezos, M., 2010. Humic acids copper binding following

722   their photochemical alteration by simulated solar light. Aquat. Geochem. 16, 207-

723   218.

724 Whitby, H., van den Berg, C.M.G., 2015. Evidence for copper-binding humic substances

725   in seawater. Mar. Chem. 173, 282–290.

726   https://doi.org/10.1016/j.marchem.2014.09.011

727 Whitby, H., Posacka, A. M., Maldonado, M.T., van den Berg, C.M.G., 2018. Copper-

728   binding ligands in the NE Pacific. Mar. Chem. 204, 36–48.

729 Whitby, H., Planquette, H., Cassar, N., Bucciarelli, E., Osburn, C.L., Janssen, D.J., Cullen,

730   J.T., González, A.G., Völker C., Sarthou, G., 2020. A call for refining the role of

731   humic-like substances in the oceanic iron cycle. Sci. Rep. 10, 6144.

732   https://doi.org/10.1038/s41598-020-62266-7

733   Wong, K.H., Obata, H., Kim, T., Wakuta, Y., Takeda, S., 2019. Distribution and

734   speciation of copper and its relationship with FDOM in the East China Sea. Mar.

735   Chem. 212, 96-107.

736   Yamashita, Y., Tanoue, E., 2003. Chemical characterization of protein-like fluorophores

737   in DOM in relation to aromatic amino acids. Mar. Chem. 82, 255–271.

738   Yang, F., Song, G., Massicotte, P., Wei, H., Xie, H., 2020. Depth-resolved photochemical

739   lability of dissolved organic matter in the western tropical Pacific Ocean. J. Geophys.

740   Res. 125, e2019JG005425.

741   Yang, R., van den Berg, C.M.G., 2009. Metal complexation by humic substances in

742   seawater. Environ. Sci. Technol. 43, 7192-7197.

743   Yoro, S.C., Panagiotopoulos, C., Sempéré, R., 1999. Dissolved organic carbon

744   contamination induced by filters and storage bottles. Water Res. 33, 1956-1959.

745

746   Figures captions

747

748   Fig. 1. Experimental design of the photodecomposition experiment.

749   Fig. 2. Hydrography at Station G1, where the deep seawater for the photodecomposition

750   experiment was collected. (A) Vertical profiles of temperature (°C, solid line, lower

751   axis), salinity (dashed line, lower axis), and chlorophyll-a fluorescence (fluorescence

752   unit, dotted line, upper axis). (B) Vertical profiles of three types of fluorescent dissolved

753   organic matter (FDOM), terrestrial humic-like substances (THS, solid square), marine

754   humic-like substances (MHS, open circle), and tyrosine protein-like substances (TYR,

755   solid triangle).

756   Fig. 3. Temporal variations of (A) three types of fluorescent dissolved organic matter

757   (FDOM) and (B) organic metal-binding ligands in the photodecomposition experiment.

758   All of the data are shown with the standard variation of triplicate samples. The dark

759   control on day 6 is shown on day 6.3 for comparison. (A) Terrestrial humic-like

760   substances (THS, solid square), marine humic-like substances (MHS, open circle), and

761   tyrosine protein-like substances (TYR, solid triangle). (B) Fe-binding ligands (FeL,

762   solid triangle), strong Cu-binding ligands (CuL$_1$, solid circle), and weak Cu-binding

763   ligands (CuL$_2$, open circle).

764   Fig. 4. Changes of terrestrial humic-like substances (THS), marine humic-like

765   substances (MHS), tyrosine protein-like substances (TYR), Fe-binding ligands (FeL),

766   and strong Cu-binding ligands (CuL$_1$) relative to the initial values in the

767   photodecomposition experiment.

768

769

770

Filtered deep seawater   Natural sunlight
500 mL × 24   25 °C

0 Day   1 Day   6 Days

Extract FDOM sample from each bottle

Stored frozen (-20 °C)

Dissolved Cu   Dissolved Fe
Cu ligands   Fe ligands

771
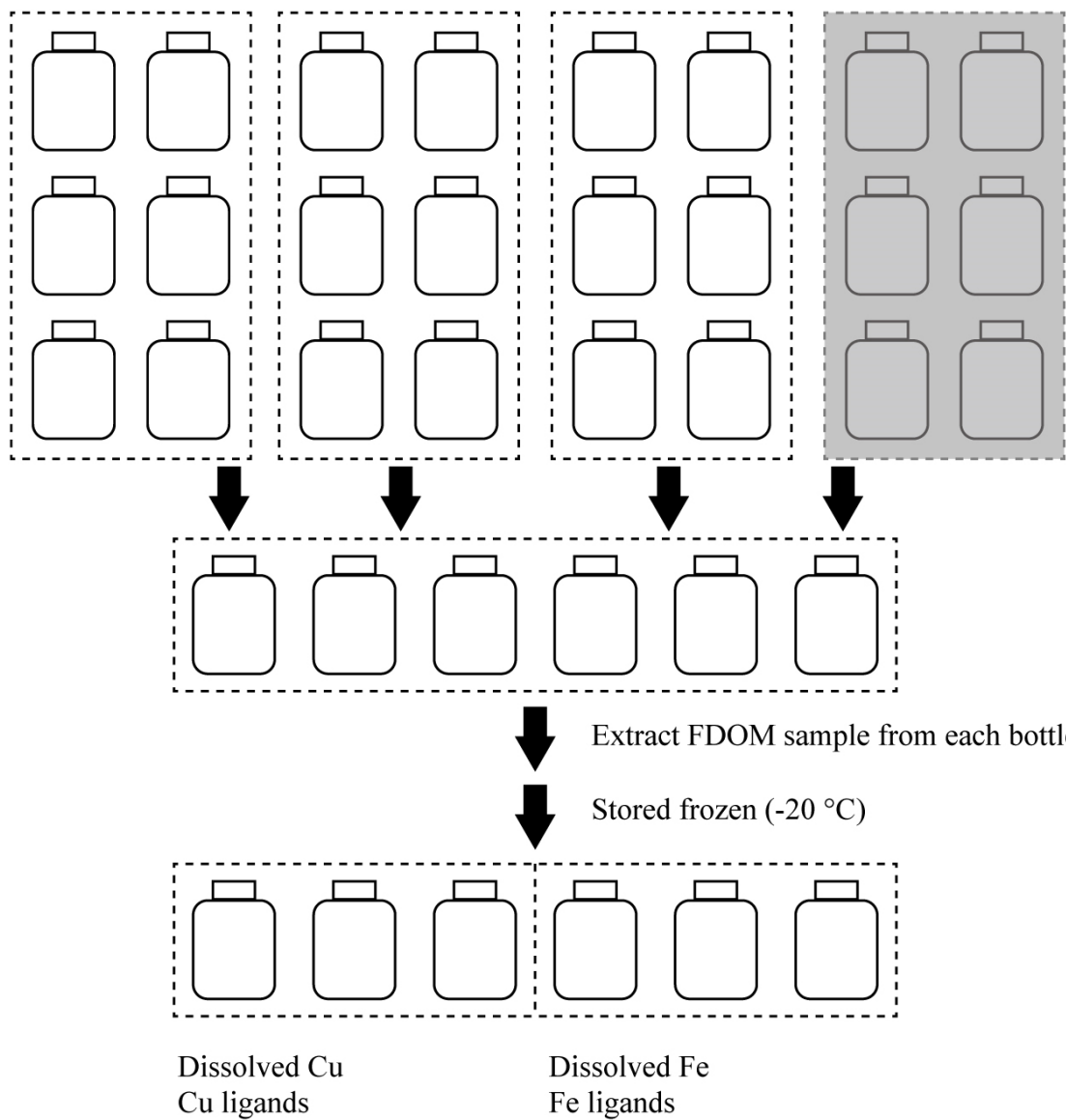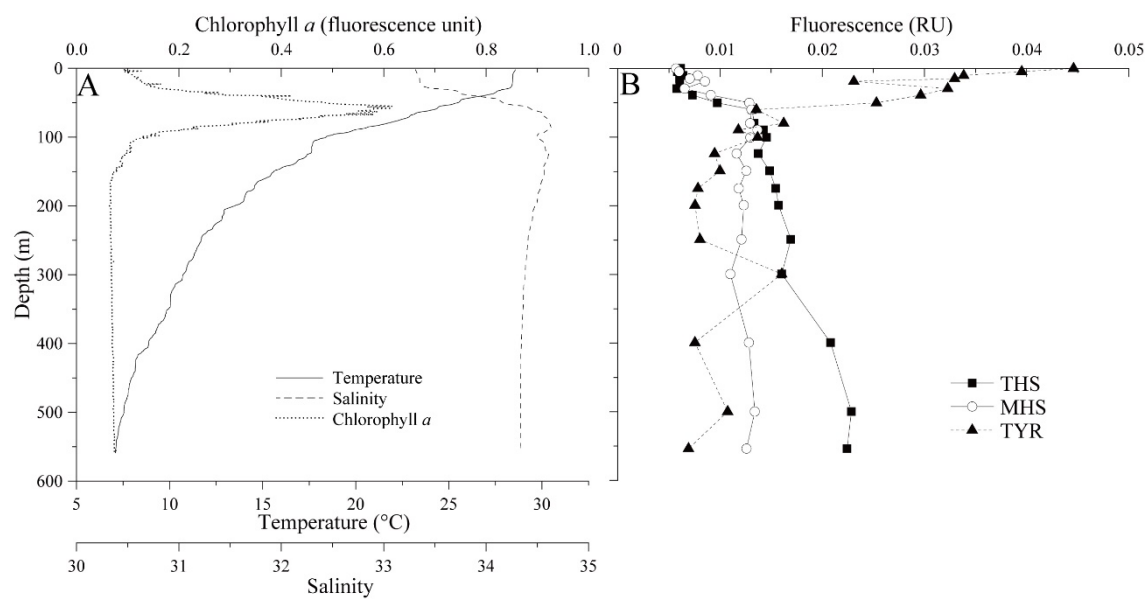
772   Fig. 1.

773

774

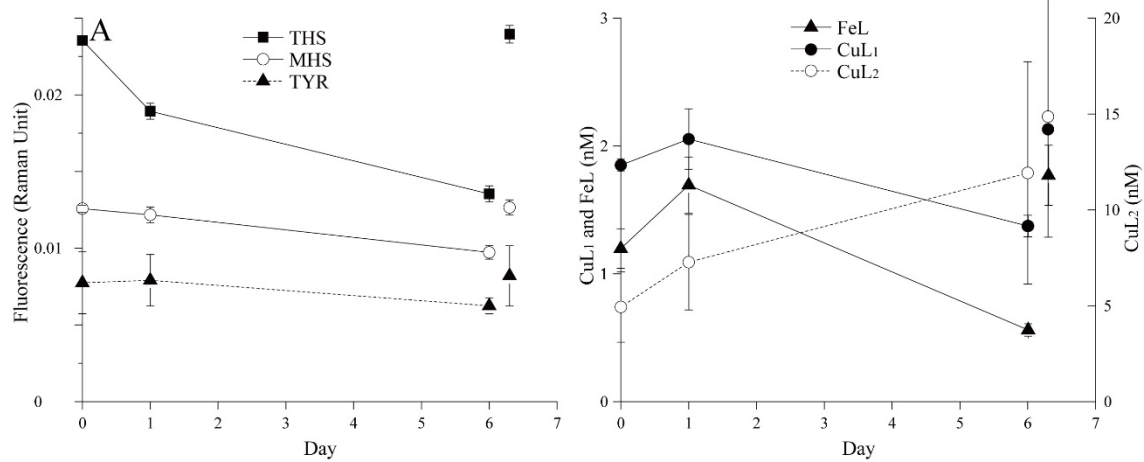775

776   Fig. 2.

777

778

779

780   Fig. 3.

781

782
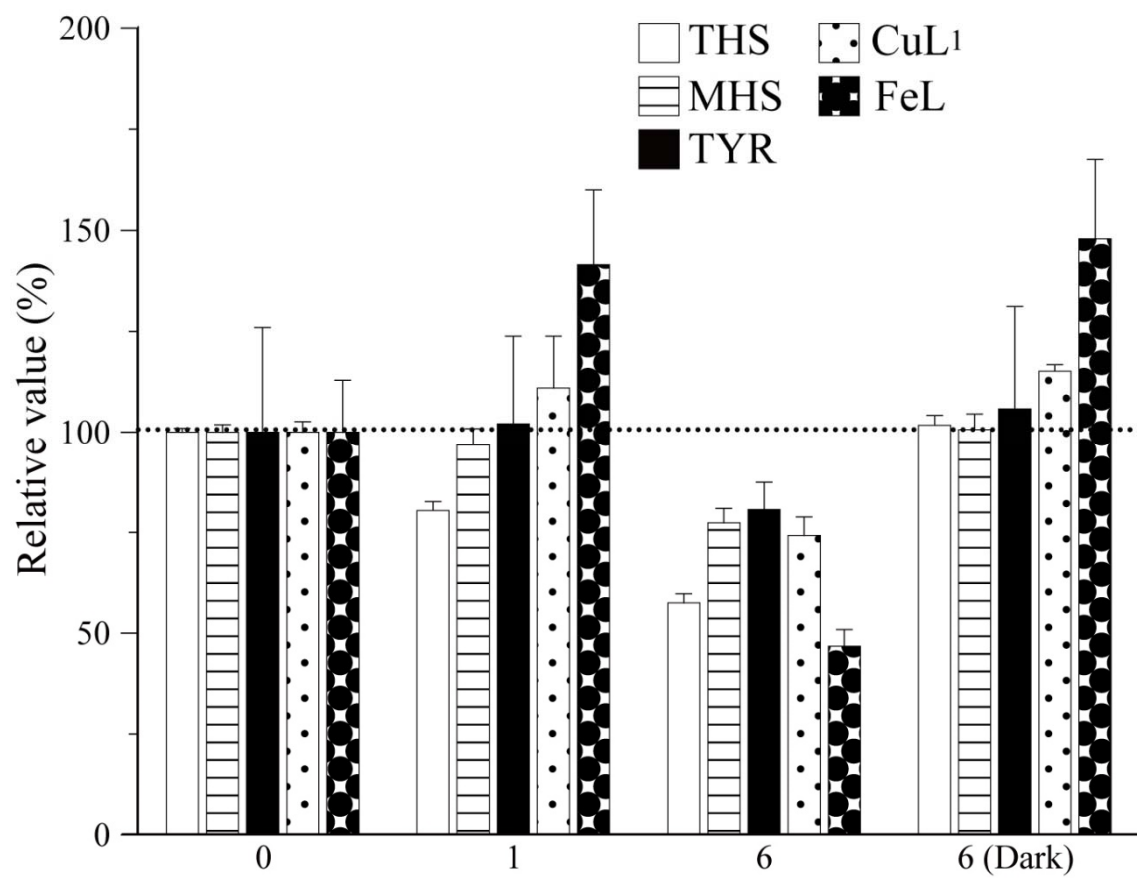
Fig. 4.

784

785   Table 1. Voltammetric parameters for Cu and Fe measurement.

	Cu	Fe
Purge time (s)	180 by N_2 gas	120 by clean air
Deposition potential (V)	−0.05	0
Deposition time (s)	120	240
Equilibration time (s)	5	15
Start potential (V)	−0.05	0
End potential (V)	−0.5	−0.85
Pulse amplitude (V)	0.025	0.035
Pulse time (s)	0.05	0.017
Voltage step (V)	0.005	0.006

786

787 Table 2. Logarithm of the conditional stability constants (M^{-1}) of organic metal-binding
788 ligands against inorganic metal ions (log $K_{M'L}$) in the photodecomposition experiment.
789

	CuL$_1$	CuL$_2$	FeL
Day 0	15.0 ± 0.2	13.0 ± 0.2	10.8 ± 0.1
Day 1	14.6 ± 0.2	12.5 ± 0.3	11.0 ± 0.1
Day 6	14.5 ± 0.1	12.0 ± 0.2	11.6 ± 0.4
Dark 6	15.1 ± 0.2	12.3 ± 0.5	11.1 ± 0.2

790